ECOHYDROLOGY
Ecohydrol. **6**, 917–926 (2013)
Published online 12 January 2012 in Wiley Online Library
(wileyonlinelibrary.com) DOI: 10.1002/eco.1245

Understanding the dynamic coupling between vegetation cover and climatic factors in a semiarid region—a case study of Inner Mongolia, China

Lei Cao,[1] Jianhua Xu,[1]* Yaning Chen,[2] Weihong Li,[2] Yang Yang,[1] Yulian Hong[1] and Zhuo Li[1]

[1] *The Research Center for East–West Cooperation in China, The Key Lab of GIScience of the Education Ministry PRC, East China Normal University, Shanghai 200062, China*

[2] *The Key Laboratory of Oasis Ecology and Desert Environment, Xinjiang Institute of Ecology and Geography, Chinese Academy of Sciences, Urumqi, Xinjiang, 830011, China*

ABSTRACT

Vegetation is sensitive to changes in the ecological environment in arid and semiarid regions, so information on the dynamics of vegetation cover changes can provide important information for ecological environmental protection and early warning of ecosystem degradation. With the SPOT/VEGETATION normalised difference vegetation index dataset of the typical semiarid land in Inner Mongolia (IM) during 1998–2008, this study applied an integrated statistical method combing asymmetric Gaussian filtering, seasonal Kendall test, R/S analysis, correlation analysis and regression analysis, to investigate the impact of climatic factors on trends in vegetation cover. The main findings are as follows: (1) Over the 1998–2008 period, the vegetation coverage is relatively stable in IM, with only 24.5% of the total area exhibiting a significant variation in cover. The spatial distribution of the vegetation cover change has the following regional characteristics: in the northeast forest region, the vegetation cover is stable; in the middle steppe region, significant changes are observed and in the southwest desert region, the vegetation exhibits significant degradation. (2) Normalised difference vegetation index time series in most regions of IM reveal a vegetation change trend. In the high vegetation covered regions, the change trend will be reversed, whereas in the low vegetation covered regions, the original change trend will be preserved. (3) Analysis of correlation coefficients and stepwise linear regression reveals relationships between vegetation change and climatic factors. Temperature and precipitation have a direct influence on vegetation change, acting as the main climatic driving forces for the regional vegetation evolution. Copyright © 2012 John Wiley & Sons, Ltd.

KEY WORDS semiarid land; vegetation coverage; NDVI; climatic factors; seasonal Kendall test; R/S analysis; stepwise regression

INTRODUCTION

Vegetation is the main part of the terrestrial ecosystem and is considered as a sensitive indicator for environmental change as it reflects land cover change to a certain extent (Beerling *et al*., 1997; Mata-González *et al*., 2011). As one of the core issues for land use/land cover change (LUCC), related studies concerning vegetation-cover change have been important for research into global change (Matthews *et al*., 2004; Pettorelli *et al*., 2005; Strengers *et al*., 2010). Furthermore, an understanding of the structure, function and relevant processes of regional vegetation cover from quantitative, spatial, temporal and multi-scale perspectives is vital in assessing vegetation dynamics (Wu and Hobbs, 2002; Aragao *et al*., 2005; Strengers *et al*., 2010). Moreover, scientists have recognised the value of evaluating spatial ecosystem patterns and temporal processes using data archives. In the past 20 years, with the development of Earth observation technology and the long-term data accumulation, researchers have the ability to analyse and discuss the vegetation coverage intensively.

Among the surface parameters extracted from the remote sensing data, the normalised difference vegetation index (NDVI) is an extensively used indicator for vegetation condition (Tucker *et al*., 2005; Beck *et al*., 2006; Brown *et al*., 2006), which is calculated as the formula NDVI = (infrared red)/(infrared + red), where infrared and red are the reflectance in the near-infrared and red electromagnetic spectrums of objects on the earth surface, respectively. NDVI is closely related to vegetation cover, phytomass, leaf area index and net primary productivity and can reflect the cover information objectively over large spatial and temporal scales. It is a particularly suitable index for evaluating the condition of vegetation growth and the spatial distribution of vegetation density (Beerling *et al*., 1997; Thuiller *et al*., 2005). By analysing the NDVI time series, it is possible to estimate inter-annual vegetation evolution trends for various vegetation attributes such as phonological changes (Moody and Johnson, 2001; Stockli and Vidale, 2004), and incorporate this information into models of climate, hydrology, net primary production and biogeochemical cycling (Yu *et al*., 2003). Currently, there are many methods for analysing NDVI time series, such as principal component analysis (Eastman and Fulk, 1993), Fourier analysis (Azzali and Menenti, 2000; Jakubauskas *et al*., 2002), wavelet decomposition (Alhamad *et al*., 2007; Martínez and Gilabert, 2009; Yang *et al*., 2011), Mann–Kendall (MK) test (Julien and

*Correspondence to: Jianhua Xu, Dept. of Geography, East China Normal University, Shanghai 200062, China.
E-mail: jhxu@geo.ecnu.edu.cn

Sobrino, 2009), texture analysis (Ricotta *et al*., 1996), and phenological measurement (Zhang *et al*., 2005). However, research documenting tests on the periodic time series for each pixel is still relatively rare.

Environmental factors, particularly the main controlling climate factors such as precipitation and temperature that affect the vegetation growth will also influence observed NDVI values (Nemani *et al*., 2003). Therefore, many studies have used NDVI to monitor vegetation response to climatic fluctuations at the regional scale (Schultz and Halpert, 1993; Wang *et al*., 2003; Fabricante *et al*., 2009; Zhong *et al*., 2010). These studies indicate that temporal variations of NDVI are closely linked with climate factors. However, our understanding of the mechanism and extent of the climatic influence on NDVI is far from complete (Wang *et al*., 2003). The interaction between temperature, radiation and water impose complex and varying limitations on vegetation activity in different parts of the world (Ni, 2011), and the development of effective methodologies for the analysis of internal mechanisms remain one of the most important and challenging issues for the remote sensing community (Bruzzone *et al*., 2003).

Inner Mongolia (IM) is ecologically typified by mid-latitudinal and semiarid temperate grassland. IM is particularly significant as it is located in the northeast China terrestrial transect, which is the typical terrestrial transect of International Geosphere–Biosphere Programme global change research and is the most sensitive area for global change (John *et al*., 2009). Owing to the drought-prone climate and human activities, the vegetation ecosystem of IM is very fragile, and both the land desertification and vegetation degradation are very severe. Many studies have confirmed that IM is one of the major dust sources in North China and East Asia (Ye *et al*., 2000; Husar *et al*., 2001; Natsagdorj *et al*., 2003). It is therefore important to understand the driving mechanisms of vegetation changes across this region. In this paper, we use high temporal resolution remote sensing images to answer two questions: (1) What are the trends of vegetation change in IM over the past 10 years? And in particular, what is driving the changes in observed vegetation patterns? (2) Can any causal relationships be found between vegetation change and climatic factors in IM?

MATERIAL AND METHODS

Study area

The IM Autonomous Region lies between the latitudes as 37°24′–53°23′N and longitudes as 97°12′–126°04′E, covering an area of 1 183 000 km^2. The major terrain is a flat plateau, with an average altitude of 1000–1500 m. The area of grassland covers 880 000 km^2, accounting for 21.7% of the total nation, and it is the largest of five large grasslands in China. The spatial distribution of IM vegetation cover (Figure 1) has the obvious characteristic of gradually diminishing from the northeast to southwest. In the eastern part, the forest and forest steppe of the Greater Higgnan Mountains has a denser vegetation cover. The western part, from west to east includes the Central Gobi, Badain Jaran Desert, Tenger Desert and Ulanbuh Desert with a land use characterised by desert and desert steppe. In the central region, the zonal vegetation types are dominated by meadow steppes, typical steppes and desert steppes (Wang *et al*., 2009a). Temperature and moisture vary longitudinally and influence the vegetation zonation. Meadow steppes are mainly distributed at the eastern end of the IM Plateau, with annual precipitation of 350–550 mm and 1800–2500 °C cumulative active temperature above 10 °C. Typical steppes are mainly distributed in the Xilingol League, where it has a semi-arid climate and an annual precipitation as 150–400 mm, being suitable for low-temperature herbaceous vegetation. Desert steppes are found primarily in the western parts of the Erleahot and Ordos regions, where annual precipitation is 150–280 mm and annual mean temperature ranges from 2.6 to 4.7 °C.

Data description

Normalised difference vegetation index data. In this research, the NDVI time series data was obtained from the Environmental and Ecological Science Data Center for West China, National Natural Science Foundation of China (http://westdc.westgis.ac.cn), covering the period from April 1998 to March 2008, consisting of 360 SPOT/VEGETATION scenes. The periods of every scene were defined as from the first to the 10th, from the 11th to the 20th, and from the 21st to the end of each month. The dataset has atmospheric correction, radiometric correction and geometric correction by the Vegetation Image Processing Center, and is processed using the maximum value composites method. This means the pixels for the syntheses are based on the selection of the maximum NDVI value during the 10 consecutive days. Then, all the pixels are set between −1 and −0.1 as −0.1, and converted to grey values as 0 ~ 255 by the formula as $DN = (i_{ndv} + 0.1)/0.004$, where DN is the grey value of the pixels, and i_{ndv} is the normalised vegetation index. To display conveniently, the grey value of every pixel is linearly stretched by $i_{ndv} = DN \times 0.004 - 0.1$, which converts the data range to between 0 and 1.

Reconstruction of normalised difference vegetation index time series. The NDVI dataset used in this study has been corrected to eliminate some interference from cloud, aerosol, solar elevation angle and surface bidirectional reflection. Nevertheless, noise effects from clouds and atmosphere are still large (Yu *et al*., 2004), which can bring about the jagged irregular fluctuations for NDVI time series. In this paper, we use asymmetric Gaussian filtering to smooth every pixel in the NDVI time series. With the premise that the growing season has a periodic character (Jonsson and Eklundh, 2002), AG filtering has a better fidelity compared with the other fitting functions (Hird and McDermid, 2009). Furthermore, this model uses the combination of segmented Gaussian functions to simulate the vegetation phenology in growing season, taking one combination as one whole growth process of vegetation. Finally, the time series is reconstructed by linking

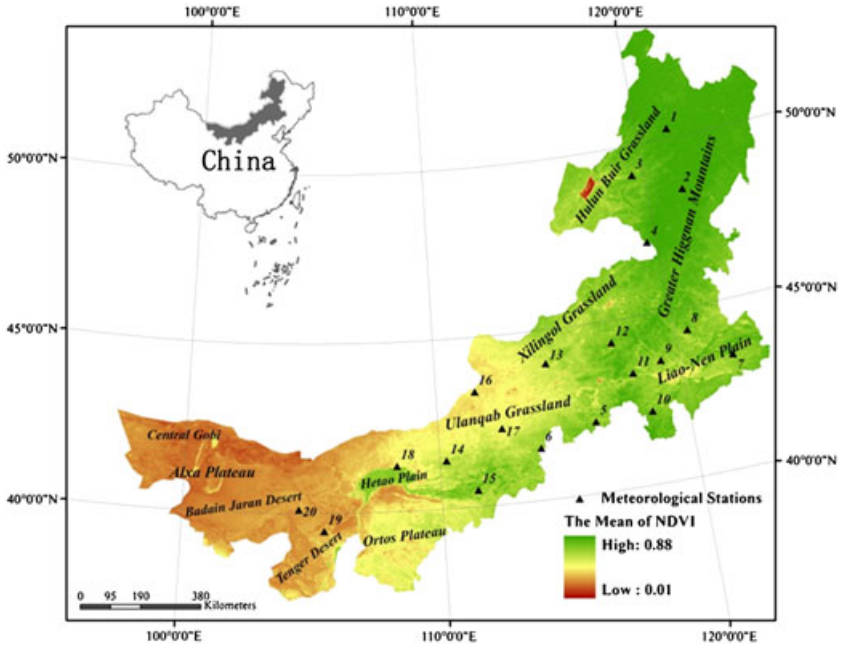

Figure 1. The location of study area.

smoothly each Gaussian fitting curve. The Gaussian fitting function can be expressed as follows:

$$g(t;x_1,x_2,\cdots,x_5)=\begin{cases}\exp\left[-\left(\dfrac{t-t_1}{x_2}\right)^{x_3}\right], & t>x_1\\ \exp\left[-\left(\dfrac{t_1-t}{x_4}\right)^{x_5}\right], & t<x_1\end{cases} \quad (1)$$

where, x_1 is the segmented inflection point of Gaussian function, which has determined the maximum or minimum of the independent time variable t in each subsection. x_2 and x_3 are the base width and steepness in the right section of the Gaussian function, x_4 and x_5 are the base width and steepness in the left section of the Gaussian function, respectively.

Climate data. The climate data used in this study was from the 10-day datasets in China ground stations of international exchange and provided by the China Meteorological Data Sharing Service System (http://cdc.cma.gov.cn). In terms of both the climate and NDVI data, the time resolution are 10 days, and the definition of time phase are from the first to the 11th, from the 11th to the 20th and from the 21st to the end of each month. Simultaneously, the two have been selected the same time series in the period of April 1998–March 2008. In other words, the time scale and the time extent for both the climate and NDVI data are totally consistent. Therefore, climate data and NDVI data are suited for each other. These stations, with different altitudes, covered a large portion of the IM from northeast to southwest. These stations were selected to represent the four major vegetation types of IM and were evenly distributed across typical vegetation areas (Table I). The vegetation map of IM was digitised from China Vegetation Map with a scale of 1 : 1 000 000.

Methodology

Three analytical tools were used for data processing. Firstly, NDVI time series trends were analysed using a seasonal Kendall test. Secondly, the long-term correlation characteristic of the NDVI time series was obtained using the rescaled range (R/S) analysis method. Finally, the quantitative relation between NDVI and its related climatic factors at the 20 stations were subjected to stepwise linear regression. Trend analysis of NDVI time series was based on pixel units, that is, we took the NDVI value of each time phase for every pixel as one time series. Grid computing was undertaken with MATLAB 7.0b (Mathworks, Natick, MA, USA) and image processing was mainly completed using ArcGIS 9.3 (Esri, Redlands, CA, USA).

Seasonal Kendall test. The MK test is generally used to examine the significance of temporal trends from time series data. Since 1945, it has been widely used to assess the significance of trends in hydrological and climate time series (Yue and Wang, 2002; Xu and Zhang, 2006; Xu *et al*., 2009). The seasonal Kendall (SK) test is a special case where the MK test is applied in the time series with periodic variation (Yu *et al*., 1993). It is preferably used to test for trends with seasonal fluctuations (Kahya and Kalayci, 2004). This test is intended to assess the randomness of a data set $X=(X_1, \ldots, X_{12})$ and $X_i=(X_{i1}, \ldots, X_{in})$ where X is a matrix of the entire monthly NDVI data over n years at a pixel. The test statistic is a sum of the Mann–Kendall statistic computed for each month. The interpretation of the rest of the test is similar to that of the MK test. With the SK test for NDVI trend testing, the null hypothesis H_0 means there is an independent distribution of data samples in the dataset X, that is, there is no change trend, whereas the optional hypothesis H_1 means that there is a change trend in the dataset X, which takes the NDVI of each pixel as a time series, SK test statistic Z and Sen's

Table I. Selected meteorological stations with their corresponding vegetation types.

No.	Station	Longitude (◦)	Latitude (◦)	Altitude(m)	Max of NDVI	Vegetation types
1	Tulihe	121.41	50.29	732.60	0.888	Forest
2	Bugt	121.55	48.46	739.7	0.888	Forest
3	Hailar	119.45	49.13	610.20	0.800	Meadow steppe
4	Arxan	119.57	47.10	1027.40	0.848	Meadow steppe
5	Duolun	116.28	42.11	1245.40	0.620	Meadow steppe
6	Huade	114.00	41.54	1482.70	0.612	Meadow steppe
7	Tongliao	122.16	43.36	178.50	0.656	Typical steppe
8	Jarud Banner	120.54	44.34	265.00	0.664	Typical steppe
9	Bairin Left Banner	119.24	43.59	484.4	0.660	Typical steppe
10	Chifeng	118.56	42.16	568.00	0.752	Typical steppe
11	Linxi	118.04	43.36	799.00	0.716	Typical steppe
12	West Ujimqin Banner	117.36	44.35	1000.60	0.652	Typical steppe
13	Abag Banner	114.57	44.01	1126.10	0.476	Typical steppe
14	Darhan United Banner	110.26	41.42	1376.60	0.412	Typical steppe
15	Hohhot	111.41	40.49	1063.00	0.644	Typical steppe
16	Erenhot	111.58	43.39	989.50	0.264	Desert steppe
17	Zhurihe	112.54	42.24	1150.80	0.316	Desert steppe
18	Urad Middle Banner	108.31	41.34	1288.00	0.224	Desert steppe
19	Jartai	105.45	39.47	1031.80	0.136	Desert steppe
20	Bayan Mod	104.48	40.1	1323.90	0.164	Desert steppe

slope β as the NDVI augment or attenuation indexes for each unit pixel.

The statistic Z of the seasonal Kendall test is expressed as follows:

$$Z = \begin{cases} \dfrac{S-1}{\sqrt{\mathrm{var}(S)}}, & S > 0 \\ 0, & S = 0 \\ \dfrac{S+1}{\sqrt{\mathrm{var}(S)}}, & S < 0 \end{cases} \tag{2}$$

where,

$$S = \sum_{i=1}^{12} S_i \tag{3}$$

$$S_i = \sum_{k=1}^{n-1} \sum_{j=k+1}^{n} \mathrm{sgn}\left(x_{ij} - x_{ik}\right) \qquad (1 \le k < j \le n) \tag{4}$$

$$\mathrm{sgn}\left(x_{ij} - x_{ik}\right) = \begin{cases} 1, & x_{ij} - x_{ik} > 0 \\ 0, & x_{ij} - x_{ik} = 0 \\ -1, & x_{ij} - x_{ik} < 0 \end{cases} \tag{5}$$

$$\mathrm{var}(S) = \sum_{i=1}^{n} n_i(n_i - 1)(2n_i + 5)/18 \tag{6}$$

where, n is month n, x_{ik} and x_{ij} are the sequential data values.

The seasonal Kendall test can be used in the following manner, for the null hypothesis H_0, $\beta = 0$, if $|Z| > Z_{(1-\alpha)/2}$, then reject the null hypothesis, where, $Z_{(1-\alpha)/2}$ is the standard normal variance, and α is the significance level for the test. When $|Z| < 1.645$, the trend variation is not significant. When $|Z| > Z_{(1-0.1)/2} = 1.645$, it means that the confidence level of this time series is less than 0.1, and the trend variation is significant. When $|Z| > Z_{(1-0.01)/2} = 2.567$, it means that the confidence level of this time series is less than 0.01, and the trend variation is highly significant. Meanwhile, $Z > 0$ reflects the increasing trend of time series. Conversely, $Z < 0$ indicates the decay trend.

Sen's slope is expressed as follows:

$$\beta = \mathrm{Median}\left(\frac{x_i - x_j}{i - j}\right) \tag{7}$$

where, $1 < j < i < n$. A positive β denotes a rising trend, whereas a negative β means a decreasing trend.

Rescaled range analysis method. Rescaled range analysis was put forward by Hurst when analysing hydrological data from the river Nile and was usually applied to analyse long-term correlation characteristics of a time series (Xu *et al*., 2004; 2010). The principle of R/S analysis is briefly introduced as follows (Mandelbrot and Wallis, 1969).

Considering a time series $X(t)$, the mean value series is defined as follows:

$$\langle x \rangle_t = \frac{1}{\tau} \sum_{t=1}^{\tau} x(t) \qquad t = 1, 2, \ldots \tag{8}$$

The accumulative deviation is

$$X(t, \tau) = \sum_{u=1}^{t} \left(x(u) - \langle x \rangle_t\right) \qquad 1 \le t \le \tau \tag{9}$$

The extreme deviation is

$$R(\tau) = \max_{1 \le t \le \tau} X(t, \tau) - \min_{1 \le t \le \tau} X(t, \tau) \tau = 1, 2, \ldots \tag{10}$$

The standard deviation is

$$S(\tau) = \left[\frac{1}{\tau} \sum_{t=1}^{\tau} \left(x(t) - \langle x \rangle_\tau\right)^2\right]^{\frac{1}{2}} \qquad \tau = 1, 2, \ldots \tag{11}$$

With the computed $R(\tau)$ and $S(\tau)$, we can obtain the formula as

$$R/S \equiv R(\tau)/S(\tau) \tag{12}$$

Supposing that,

$$R/S \propto \left(\frac{\tau}{2}\right)^H \tag{13}$$

It indicates that this time series exhibits the Hurst phenomenon, where H is the Hurst exponent. According to ($\ln\tau/2$, $\ln(R/S)$), H can be obtained by the least square method in a log-log grid, and different values of H mean that the sequence has different change trends. Hurst (1965) showed that if $\{X(t)\}$ is an independently random series with limited variance, the exponent $H = 0.5$. When $H = 0.5$, it indicates that there is no correlation or only a short-range correlation in the process. When $H > 0.5$, it means that the process has a long-enduring characteristic, and the future trend of the time series will be consistent with the past. In other words, if the past showed an increasing trend, the future will also show an increasing trend. When $H < 0.5$, it means that the process has an anti-persistence characteristic, and the future trend of the time series will be opposite from the past. In other words, if the past showed an increasing trend, the future will assume a reducing trend.

Correlation and regression analysis. Correlation is one of the most common and most useful statistical methods, which is a statistical measurement of the relationship between two variables (Zimmerman, 1986). Possible correlations range is from +1 to −1. A zero correlation indicates that there is no relationship between the variables. A negative correlation indicates that as one variable goes up, the other goes down. A positive correlation indicates that both variables move in the same direction together. Commonly, testing the significance of the correlation coefficient employs the t distribution.

In this study, correlation analysis was used to check for relations between NDVI and related climate factors such as temperature and precipitation. This paper also conducted a stepwise linear regression analysis to examine the response of the NDVI to regional climate change. In statistics, stepwise regression includes regression models in which the choice of independent variables is carried out by an automatic procedure. Stepwise regression can be achieved either by trying out the variables one by one and including them if they are statistically significant (forward selection), or by including all potential independent variables in the model and eliminating those that are not statistically significant (backward elimination), or by a combination of both methods. In our study, the forward selection method was adopted. At each stage in the process, after a new variable is added, a test is made to check if some variables can be deleted without appreciably increasing the residual sum of squares. The procedure terminates when the measure is (locally) maximised.

The multiple linear regression model is

$$\mathrm{Y} = a_0 + a_1X_1 + a_2X_2 + \ldots + a_nX_n \tag{14}$$

where, Y is a dependent variable, a_i is the coefficient of the independent variables X_i.

RESULT AND DISCUSSION

Normalised difference vegetation index change trend

With the SK test, the spatial pattern of statistic Z for NDVI in IM during 1998–2008 was obtained by calculating statistic Z of NDVI time series for each pixel. Taking significance levels as 0.1 and 0.01, the vegetation change trend was divided into five types (Figure 2), including highly significant deterioration ($Z \le -2.567$), significant deterioration ($-2.567 < Z \le -1.645$), no significance ($-1.645 < Z < 1.645$), significant improvement ($1.645 \le Z$ 2.567) and highly significant improvement ($Z \ge 2.567$).

Seasonal Kendall test results show that linear trends of NDVI change are not significant in most parts of IM, and only 24.5% of the vegetation cover showed significant change trends. Only 13.6% of the total area has a significant or highly significant deteriorated trend, and 10.9% of the total area showed significant or highly significant improvement (Table II). On balance, there is a slight tendency for overall condition of vegetation in IM to be deteriorating over the last 10 years. Of more importance however, is that about 6% of IM exhibits vegetation degradation over the past 10 years, and the regions identified should undertake urgent continuous vegetation change monitoring and apply many effective measures to reverse the degradation of vegetation.

The spatial distribution of significant change in NDVI has distinct regional characteristics. In the northeast, forest and meadow steppes of the Greater Higgnan Mountains are the main feature, and the vegetation coverage is relatively high. In this district, areas exhibiting significant change in the NDVI time series are extremely small, mainly sporadically located in the middle section of Greater Higgnan Mountains and the Hulun Buir Grassland. However, in the southwest desert area to the west of the Hetao Plain, there is a marked increase in pixels exhibiting significant changes in NDVI. The areas of significant decline are patchy in the north of Alxa Plateau, whereas improved areas are scattered in the south edge of the Badan Jaran Desert and in the north edge of Tengger Desert. These changes suggest that the vegetation coverage is unstable, and the overall trend is mainly towards degradation. In the central region, mainly covered by typical steppes and arid grasslands, the grids with significant NDVI change have cluster-like distributions. Significant and highly significant improved areas are concentrated in the Keerqin Sandy Land and Ortos Plateau, which are historically areas with serious desertification. The desertification control project in this region has achieved remarkable results since 1998, with increased vegetation and improved ecological condition in Keerqin Sandy Land, Muus Sandy Land and Kubuqi Desert (Chang *et al*., 2009; Na *et al*., 2010; Wang *et al*., 2010). The vegetation exhibiting significant and highly significant decrease in NDVI mostly appears in the steppe, especially

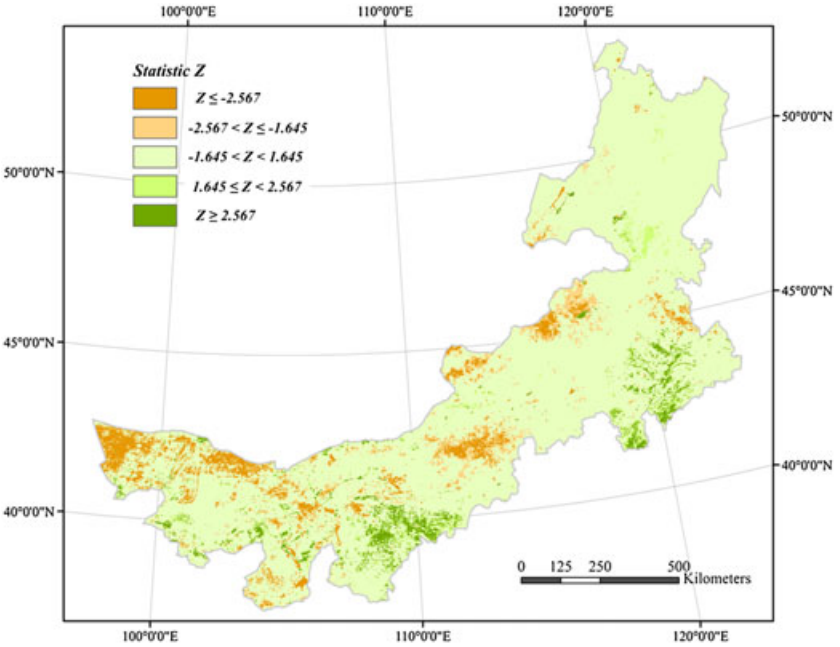

Figure 2. Spatial pattern of seasonal Kendall test statistic Z for normalised difference vegetation index in Inner Mongolia during 1998–2008.

Table II. Area and proportion of land in Inner Mongolia exhibiting a specific significant vegetation trend.

Vegetation variation trend		Area (km^2)	Proportion
Deterioration	Highly significant	70443.4	5.95%
	Significant	90920.2	7.69%
Improvement	Significant	83528.1	7.06%
	Highly significant	45516.7	3.85%

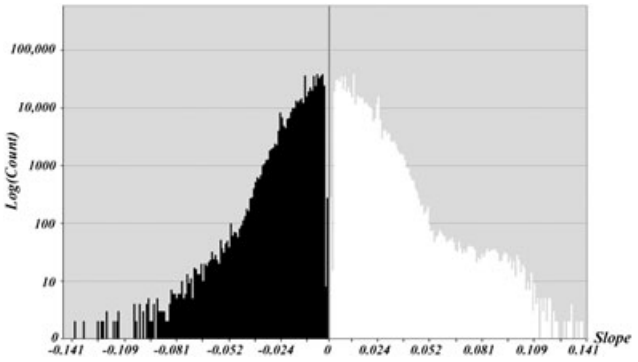

Figure 3. Sen's slope β histogram for normalised difference vegetation index series in Inner Mongolia in 1998–2008.

in the Xilingol Grassland and Ulanqab Grassland. It is well known that the ecosystem of these typical steppe regions is very sensitive and fragile, and irrational animal husbandry production, sharply increased population and rapid urbanisation have brought pressures leading to vegetation degradation (Ma *et al*., 2007; Wang *et al*., 2009b; Liu *et al*., 2010).

The Sen's slope β histogram (Figure 3) is constructed from all the pixels in the study area, where horizontal axis is the value of β, standing for enhancement, attenuation and no obvious change when the values are greater than 0, less than 0 and equal to 0, respectively. To display conveniently, the vertical axis is the natural logarithm of the pixel number. The results show that enhancement is observed in 30.4% of the total pixels and attenuation in 31.9% of the total pixels. Overall, this results in a regional balance over the 10-year period without a large area of decay.

Future trend of normalised difference vegetation index

With the R/S analysis method, the spatial distribution of Hurst exponents in IM over 1998–2008 (Figure 4) can be obtained by calculating Hurst exponent (H) of NDVI time series for every pixel. Taking $H = 0.5$ as the critical threshold, the characteristics of future vegetation change trend can be divided into three types, that is, $H = 0.5$ indicates that future vegetation change is random without an obvious change trend, $H > 0.5$ means that future vegetation change is consistent with the present one, which can be called persistence, and $H < 0.5$ shows that future vegetation change is in contrast with the present one, which can be called anti-persistence.

Statistical analysis indicates that NDVI time series in most regions of IM are not Markov processes, but exhibit a particular tendency. Vegetation variation exhibiting a persistence characteristic is observed in 64.7% of the total area, and vegetation variation exhibiting anti-persistence covers 35.1% of the total area. The Hurst exponent is generally higher in west and trends lower in the east. Pixels with H values less than 0.5 are mainly observed on the Greater Higgnan Mountains and Hetao plain, indicating that the vegetation change trend in the future is opposite to the present situation. In other regions, the H values exceed 0.5, indicating persistence. Pixels with H values between 0.5 and 0.7 are mainly located in the typical steppe and desert steppe, and

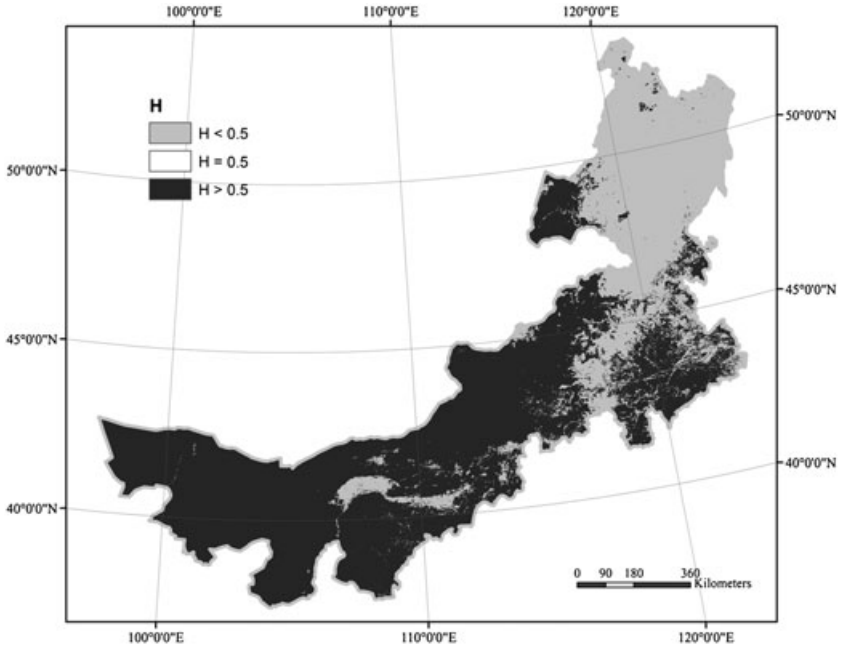

Figure 4. The spatial distribution of Hurst exponents of normalised difference vegetation index time series in Inner Mongolia in 1998–2008.

pixels with H values greater than 0.7 are mainly situated in the Otindag Sandy Land and desert area in the west. These results indicate that the vegetation cover condition has a close relationship with the vegetation change trend.

Here, according to the mean of NDVI (MNDVI) in descending order, all the pixels are divided to five classes (Table III). It can be seen from Table III that Hurst exponent for NDVI time series has negative correlation with the mean value of MNDVI, indicating that regions with poor vegetation cover tend to show as persistence, and the regions with good vegetation cover tend to show as anti-persistence. Similar results were reported by Wang *et al* (2005). This result indicates that the vegetation change trend in the poor ecological environments is more stable and is difficult to improve. Therefore, in these regions, it is important to maintain the vegetation growth trend to ensure the continuous improvement of the ecological environment.

Climate influences on the vegetation variation trend

Many studies have shown that vegetation is sensitive to regional climatic fluctuations (Fabricante *et al*., 2009; Zhong *et al*., 2010; Xu *et al*., 2011; Yang *et al*., 2011). In order to investigate the relationships between NDVI and regional climate factors in IM, the mean values of NDVI at the pixel nearest 20 selected meteorological stations, listed in Table I, were extracted from the SPOT vegetation images, and then correlation analyses were performed on the basis of the times series of 372 data among NDVI, precipitation (P), temperature (T), relative humidity (H) and sunshine hours (S). Results are reported in Table IV and show that overall, the relation between NDVI and temperature and NDVI and precipitation are the strongest. Weaker relations are found with sunshine hours and relative humidity.

To describe the effect of climatic factors on NDVI, and weaken the interaction between the four measured climatic factors, stepwise linear regression has been performed in Table V. Results show that among the four climate factors, temperature and precipitation were entered and sunshine hours and relative humidity were removed during the automatic selection of independent variables at most of the selected stations. The reason is that the sunshine hours can be directly reflected by temperature and relative humidity can be affected by precipitation, so the latter two are not independent variables.

Abundant precipitation was very stable in the forest vegetation zone, and scarce precipitation was stable in the desert steppe vegetation zones. The resulting contribution of these zones to the NDVI change was statistically weak as a result. Therefore, the precipitation variables of seven stations were removed or replaced by relative humidity with similar ecological significance. For all other stations,

Table III. Statistical characteristics for Hurst exponents under different vegetation covers.

Pixels' class	MNDVI range	MNDVI average	Mean H	Proportion for $H < 0.5$(%)	Proportion for $H > 0.5$(%)
1	0 –0.2	0.11	0.8251	0.08	99.90
2	0.2–0.4	0.29	0.6304	2.65	97.35
3	0.4–0.6	0.51	0.5550	21.26	78.74
4	0.6–0.8	0.70	0.4672	71.84	28.16
5	0.8–1	0.83	0.4088	99.41	0.59

Table IV. Correlation coefficients of normalised difference vegetation index versus climatic factors.

No.	Station	NDVI vs P	NDVI vs T	NDVI vs H	NDVI vs S	Vegetation types
1	Tulihe	0.606**	0.864**	0.277**	0.375**	Forest
2	Bugt	0.499**	0.876**	0.253**	0.363**	Forest
3	Hailar	0.489**	0.857**	−0.323**	0.548**	Meadow steppe
4	Arxan	0.575**	0.874**	0.071	0.422**	Meadow steppe
5	Duolun	0.539**	0.846**	0.195**	0.222**	Meadow steppe
6	Huade	0.493**	0.726**	0.115*	0.308**	Meadow steppe
7	Tongliao	0.428**	0.754**	0.549**	0.189**	Typical steppe
8	Jarud Banner	0.340**	0.694**	0.568**	0.097	Typical steppe
9	Bairin Left Banner	0.328**	0.634**	0.574**	0.365**	Typical steppe
10	Chifeng	0.462**	0.712**	0.620**	0.352**	Typical steppe
11	Linxi	0.481**	0.788**	0.531**	0.390**	Typical steppe
12	West Ujimqin Banner	0.473**	0.851**	−0.110*	0.519**	Typical steppe
13	Abag Banner	0.436**	0.789**	−0.341**	0.501**	Typical steppe
14	Darhan United Banner	0.480**	0.754**	−0.048	0.316**	Typical steppe
15	Hohhot	0.515**	0.721**	0.228**	0.381**	Typical steppe
16	Erenhot	0.297**	0.600**	−0.349**	0.369**	Desert steppe
17	Zhurihe	0.456**	0.696**	−0.075	0.414**	Desert steppe
18	Urad Middle Banner	0.340**	0.721**	−0.234**	0.505**	Desert steppe
19	Jartai	0.154**	0.573**	−0.182**	0.371**	Desert steppe
20	Bayan Mod	0.157**	0.415**	−0.179**	0.267**	Desert steppe

*Correlation is significant at the 0.05 level (2-tailed).
**Correlation is significant at the 0.01 level (2-tailed).
Note: NDVI, normalised difference vegetation index, 10-day maximum NDVI; H, 10-day average relative humidity; P, 10-day average precipitation; T, 10-day annual temperature; α, Significance level.

Table V. Stepwise linear regression equations describing the relationship between normalised difference vegetation index and climatic factors.

No.	Station	Regression equation	R^2	F	α
1	Tulihe	NDVI = 0.00150T + 0.00802H − 0.1834	0.829	893	0.001
2	Bugt	NDVI = 0.00181T + 0.00540H + 0.0162	0.814	808	0.001
3	Hailar	NDVI = 0.00107T + 0.00017P + 0. 2148	0.744	537	0.001
4	Arxan	NDVI = 0.00139T + 0.00028P + 0.2831	0.629	316	0.001
5	Duolun	NDVI = 0.00079T + 0.00011P + 0.2019	0.734	508	0.001
6	Huade	NDVI = 0.00061T + 0.00015P + 0.1678	0.553	228	0.001
7	Tongliao	NDVI = 0.00076T + 0.00010P + 0.1999	0.582	257	0.001
8	Jarud Banner	NDVI = 0.00065T + 0.00005P + 0.1914	0.487	175	0.001
9	Bairin Left Banner	NDVI = 0.00064T + 0.00004P + 0.2048	0.406	126	0.001
10	Chifeng	NDVI = 0.00082T + 0.00014P + 0.1843	0.520	200	0.001
11	Linxi	NDVI = 0.00090T + 0.00013P + 0.2251	0.641	329	0.001
12	West Ujimqin Banner	NDVI = 0.00102T + 0.00012P + 0.1896	0.733	506	0.001
13	Abag Banner	NDVI = 0.00051T + 0.00008P + 0.1456	0.631	316	0.001
14	Darhan United Banner	NDVI = 0.00040T + 0.00011P + 0.1328	0.590	265	0.001
15	Hohhot	NDVI = 0.00074T + 0.00019P + 0.1399	0.568	242	0.001
16	Erenhot	NDVI = 0.00017T + 0.1055	0.360	208	0.001
17	Zhurihe	NDVI = 0.00037T + 0.00108H + 0.0675	0.528	347	0.001
18	Urad Middle Banner	NDVI = 0.00019T + 0.0998	0.520	400	0.001
19	Jartai	NDVI = 0.00009T + 0.0808	0.328	181	0.001
20	Bayan Mod	NDVI = 0.00007T + 0.0734	0.172	77	0.001

Note: NDVI, normalised difference vegetation index, 10-day maximum NDVI; H, 10-day average relative humidity; P, 10-day average precipitation; T, 10-day annual temperature; α, significance level.

the variables of temperature and precipitation were entered during the step linear regression. The tabulated results indicate that each regression model was statistically significant at 0.001 levels and gave positive correlations between NDVI and precipitation and temperature. These results support the conclusion that temperature and precipitation have a direct impact on vegetation change and influence the evolution of regional vegetation.

CONCLUSIONS

With seasonal Kendall test and R/S analysis for the NDVI time series of each pixel, we produced spatial distribution maps of statistic Z and Hurst exponent and analysed the evolution trends of the IM vegetation coverage in the period of 1998–2008. A stepwise linear regression model was then used for exploring the causality relationship

between NDVI and climatic factors, and temperature and precipitation were extracted as the principal climate driver forces affecting the vegetation changes. According to the analytic results, interpretation and discussions presented, we may come to the following conclusions:

(1) Over the 10-year period (1998–2008), the vegetation cover is relatively stable in IM, with only 24.5% of the total area showing a significant variation trend in vegetation cover. From northeast to southwest, the vegetation condition becomes gradually worse, and the areas with significant vegetation change increase. The spatial distribution of the areas with significant vegetation change has the following regional characteristics: the vegetation cover is stable in the northeast, with significant changes concentrated in the middle region and in the southwest, where the trend is towards degradation. In the central part, the governance in the key regions of desertification appears to have been highly effective, but in steppe regions, grassland degradation is more serious and will require continuous monitoring for vegetation change, and implementation of measures to effectively control the decay of vegetation.
(2) Applying the Hurst index to NDVI time series reveals that most regions of IM have a change trend. The dominant trend is towards persistence (64.7% of the total area), and vegetation variation exhibiting anti-persistence over 35.1% of the total area. The spatial distribution of Hurst exponent exhibits a trend of high in west whereas low in east'. Moreover, the H value has a negative correlation with NDVI, indicating that the vegetation change trend in the high vegetation covered regions will be reversed, whereas that in the low vegetation covered regions will keep the original change trend. So, once the vegetation in the poor ecological environment shows the decreased or increased trend, it will maintain the inertia without change in a short time.

The correlation analyses show that the relationships between NDVI and temperature and between NDVI and precipitation are the most significant, and weaker relationships are found between sunshine hours and relative humidity. In the stepwise linear regression analyses, temperature and precipitation have entered into the equation, whereas sunshine hours and relative humidity have been rejected at most of the selected stations. With the analysis on the correlation coefficient and stepwise linear regression model, it is indicated that there is a close relationship between vegetation change and climatic factors, and the temperature and precipitation have direct impact on vegetation change, acting as the main climatic driving forces for the regional vegetation evolution.

ACKNOWLEDGEMENTS

This work was supported by National Basic Research Program of China (973 Program; No: 2010CB951003) and National Natural Science Foundation of China (Grant No. 41040015). The authors are very grateful to Professor Keith Smettem and the anonymous referees for their hard work and generous comments given for the improvement of the manuscript.

REFERENCES

Alhamad MN, Stuth J, Vannucci M. 2007. Biophysical modelling and NDVI time series to project near-term forage supply: spectral analysis aided by wavelet denoising and ARIMA modelling. *International Journal of Remote Sensing* **28**: 2513–2548. doi: 10.1080/01431160600954670

Aragao L, Shimabukuro YE, Santo F, Williams M. 2005. Landscape pattern and spatial variability of leaf area index in Eastern Amazonia. *Forest Ecology and Management* **211**: 240–256. doi: 10.1016/j.foreco.2005.02.062

Azzali S, Menenti M. 2000. Mapping vegetation–soil–climate complexes in southern Africa using temporal Fourier analysis of NOAA-AVHRR NDVI data. *International Journal of Remote Sensing* **21**: 973–996. doi: 10.1080/014311600210380

Beck PSA, Atzberger C, Hogda KA, Johansen B, Skidmore AK. 2006. Improved monitoring of vegetation dynamics at very high latitudes: a new method using MODIS NDVI. *Remote Sense of Environment* **100**: 321–334. doi: 10.1016/j.rse.2005.10.021

Beerling DJ, Woodward FI, Lomas M, Jenkins AJ. 1997. Testing the responses of a dynamic global vegetation model to environmental change: a comparison of observations and predictions. *Global Ecology and Biogeography* **6**: 439–450. doi: 10.2307/2997353

Brown ME, Pinzon JE, Didan K, Morisette JT, Tucker CJ. 2006. Evaluation of the consistency of long-term NDVI time series derived from AVHRR, SPOT-Vegetation, SeaWiFS, MODIS, and Landsat ETM+ sensors. *IEEE Transactions on Geoscience and Remote Sensing* **44**: 1787–1793. doi: 10.1109/tgrs.2005.860205

Bruzzone L, Smits PC, Tilton JC (2003) Foreword—Special issue on analysis of multitemporal remote sensing images. *IEEE Transactions on Geoscience and Remote Sensing* **41**: 2419–2422. doi: 10.1109/tgrs.2003.820004

Chang X, Cai M, Zhang J, Li J. 2009. Effect of artificial afforestation on desertification in typical area of Horqin Sandy Land. *Journal of Desert Research* **29**: 611–616.

Eastman JR, Fulk M. 1993. Long sequence time series evaluation using standardized principal components. *Photogrammetric Engineering and Remote Sensing* **59**: 1307–1312.

Fabricante I, Oesterheld M, Paruelo JM. 2009. Annual and seasonal variation of NDVI explained by current and previous precipitation across Northern Patagonia. *Journal of Arid Environments* **73**: 745–753. doi: 10.1016/j.jaridenv.2009.02.006

Hird JN, McDermid GJ. 2009. Noise reduction of NDVI time series: an empirical comparison of selected techniques. *Remote Sensing of Environment* **113**: 248–258. doi: 10.1016/j.rse.2008.09.003

Hurst HE (ed). 1965. Long-term Storage: An Experimental Study. Constable: London.

Husar RB, Tratt DM, Schichtel BA. 2001. Asian dust events of April 1998. *Journal of Geophysical Research-Atmospheres* **106**: 18317–18330. doi: 10.1029/2000JD900788

Jakubauskas ME, Legates DR, Kastens JH. 2002. Crop identification using harmonic analysis of time-series AVHRR NDVI data. *Computers and Electronics in Agriculture* **37**: 127–139. doi: 10.1016/S0168-1699(02)00116-3

John R, Chen JQ, Lu N, Wilske B. 2009. Land cover/land use change in semi-arid Inner Mongolia: 1992–2004. *Environmental Research Letters* **4**. doi: 045010 10.1088/1748-9326/4/4/045010

Jonsson P, Eklundh L. 2002. Seasonality extraction by function fitting to time-series of satellite sensor data. *IEEE Transactions on Geoscience and Remote Sensing* **40**: 1824–1832. doi: 10.1109/tgrs.2002.802519

Julien Y, Sobrino JA. 2009. Global land surface phenology trends from GIMMS database. *International Journal of Remote Sensing* **30**: 3495–3513. doi: 10.1080/01431160802562255

Kahya E, Kalayci S. 2004. Trend analysis of streamflow in Turkey. *Journal of Hydrology* **289**: 128–144. doi: 10.1016/j.jhydrol.2003.11.006

Liu S, Wang T, Guo J, Qu J, An P. 2010. Vegetation change based on SPOT-VGT data from 1998–2007, northern China. *Environmental Earth Sciences* **60**: 1459–1466. doi: 10.1007/s12665-009-0281-4

Ma S, Wang T, Xue X. 2007. Dynamic changes of desertification land in the Northern Xilinguole grassland. *Journal of Arid Land Resources and Environment* **21**: 77–82.

Mandelbrot BB, Wallis JR. 1969. Robustness of the rescaled range R/S in the measurement of noncyclic long-run statistical dependence. *Water Resources Research* **5**: 967–988.

Martínez B, Gilabert MA. 2009. Vegetation dynamics from NDVI time series analysis using the wavelet transform. *Remote Sensing of Environment* **113**: 1823–1842. doi: 10.1016/j.rse.2009.04.016

Mata-González R, Martin DW, McLendon T, Trlica MJ, Pearce RA. 2011. Invasive plants and plant diversity as affected by groundwater depth and microtopography in the Great Basin. *Ecohydrology*: Online first, 25 Aug 2011. doi: 10.1002/eco.252

Matthews HD, Weaver AJ, Meissner KJ, Gillett NP, Eby M. 2004. Natural and anthropogenic climate change: incorporating historical land cover change, vegetation dynamics and the global carbon cycle. *Climate Dynamics* **22**: 461–479. doi: 10.1007/s00382-004-0392-2

Moody A, Johnson DM. 2001. Land-surface phenologies from AVHRR using the discrete Fourier transform. *Remote Sensing of Environment* **75**: 305–323. doi: 10.1016/S0034-4257(00)00175-9

Na Y, Wulan T, Qin FY. 2010. Dynamic monitoring of Horqin sandy land desertification based on 3S techniques. *Journal of Arid Land Resources and Environment* **24**: 50–54.

Natsagdorj L, Jugder D, Chung YS. 2003. Analysis of dust storms observed in Mongolia during 1937–1999. *Atmospheric Environment* **37**: 1401–1411. doi: 10.1016/s1352-2310(02)01023-3

Nemani RR, Keeling CD, Hashimoto H, Jolly WM, Piper SC, Tucker CJ, Myneni RB, Running SW. 2003. Climate-driven increases in global terrestrial net primary production from 1982 to 1999. *Science* **300**: 1560–1563. doi: 10.1126/science.1082750

Ni J. 2011. Impacts of climate change on Chinese ecosystems: key vulnerable regions and potential thresholds. *Regional Environmental Change* **11**: S49-S64. doi: 10.1007/s10113-010-0170-0

Pettorelli N, Vik JO, Mysterud A, Gaillard JM, Tucker CJ, Stenseth NC. 2005. Using the satellite-derived NDVI to assess ecological responses to environmental change. *Trends in Ecology & Evolution* **20**: 503–510. doi: 10.1016/j.tree.2005.05.011

Ricotta C, Avena GC, Ferri F. 1996. Analysis of human impact on a forested landscape of central Italy with a simplified NDVI texture descriptor. *International Journal of Remote Sensing* **17**: 2869–2874. doi: 10.1080/01431169608949112

Schultz PA, Halpert MS. 1993. Global correlation of temperature, NDVI and precipitation. *Advances in Space Research* **13**: 277–280. doi: 10.1016/0273-1177(93)90559-T

Stockli R, Vidale PL. 2004. European plant phenology and climate as seen in a 20-year AVHRR land-surface parameter dataset. *International Journal of Remote Sensing* **25**: 3303–3330. doi: 10.1080/01431160310001618149

Strengers BJ, Muller C, Schaeffer M, Haarsma RJ, Severijns C, Gerten D, Schaphoff S, van den Houdt R, Oostenrijk R. 2010. Assessing 20th century climate–vegetation feedbacks of land-use change and natural vegetation dynamics in a fully coupled vegetation–climate model. *International Journal of Climatology* **30**: 2055–2065. doi: 10.1002/joc.2132

Thuiller W, Lavorel S, Araujo MB, Sykes MT, Prentice IC. 2005. Climate change threats to plant diversity in Europe. *Proceedings of the National Academy of Sciences of the USA* **102**: 8245–8250. doi: 10.1073/pnas.0409902102

Tucker CJ, Pinzon JE, Brown ME, Slayback DA, Pak EW, Mahoney R, Vermote EF, El Saleous N. 2005. An extended AVHRR 8-km NDVI dataset compatible with MODIS and SPOT vegetation NDVI data. *International Journal of Remote Sensing* **26**: 4485–4498. doi: 10.1080/01431160500168686

Wang H, Li X, Long H, Zhu W. 2009a. A study of the seasonal dynamics of grassland growth rates in Inner Mongolia based on AVHRR data and a light-use efficiency model. *International Journal of Remote Sensing* **30**: 3799–3815. doi: 10.1080/01431160802552702

Wang H, Li Z, Han G. 2009b. Spatial distribution and temporal changing of vegetation cover in Xilinguole steppe region. *Ecology and Environmental Sciences* **18**: 1472–1477.

Wang J, Rich PM, Price KP. 2003. Temporal responses of NDVI to precipitation and temperature in the central Great Plains, USA. *International Journal of Remote Sensing* **24**: 2345–2364. doi: 10.1080/01431160210154812

Wang X, Wang C, Niu Z. 2005. Application of R/S Method in Analyzing NDVI Time Series. *Geography and Geo-Information Science* **21**: 20–23.

Wang Zl, Zhi Y, Li Z. 2010. Parallel analysis on vegetation landscape pattern of different eco-functional areas in Dongsheng region of Erdos. *Journal of Anhui University (Natural Science Edition)* **34**: 101–108.

Wu JG, Hobbs R. 2002. Key issues and research priorities in landscape ecology: an idiosyncratic synthesis. *Landscape Ecology* **17**: 355–365. doi: 10.1023/A:1020561630963

Xu JH, Lu Y, Su FL, Ai NS. 2004. R/S and wavelet analysis on the evolutionary process of regional economic disparity in China during the past 50 years. *Chinese Geographical Science* **14**: 193–201. doi: 10.1007/s11769-003-0047-y

Xu JH, Chen YN, Li WH, Ji MH, Dong S, Hong YL. 2009. Wavelet analysis and nonparametric test for climate change in Tarim River Basin of Xinjiang during 1959–2006. *Chinese Geographical Science* **19**: 306–313. doi: 10.1007/s11769-009-0306-7

Xu JH, Li WH, Ji MH, Lu F, Dong S. 2010. A comprehensive approach to characterization of the nonlinearity of runoff in the headwaters of the Tarim River, western China. *Hydrological Processes* **24**: 136–146. doi: 10.1002/hyp.7484

Xu JH, Chen YN, Lu F, Li WH, Zhang LJ, Hong YL. 2011. The nonlinear trend of runoff and its response to climate change in the Aksu River, western China. *International Journal of Climatology* **31**: 687–695. doi: 10.1002/joc.2110

Xu Z, Zhang N. 2006. Long-term trend of precipitation in the Yellow River basin during the past 50 years. *Geographical Research* **25**: 27–34.

Yang Y, Xu JH, Hong YL, Lv GH. 2011. The dynamic of vegetation coverage and its response to climate factors in Inner Mongolia, China. *Stochastic Environmental Research and Risk Assessment*: Online first, 23 April 2011. doi: 10.1007/s00477-011-0481-9

Ye D, Chou J, Liu J. 2000. Causes of sand-stormy weather in northern China and control measures. *Acta Geographica Sinica* **55**: 513–521.

Yu FF, Price KP, Ellis J, Kastens D. 2004. Satellite observations of the seasonal vegetation growth in central Asia: 1982–1990. *Photogrammetric Engineering and Remote Sensing* **70**: 461–469. doi: 0099-1112/04/7004

Yu FF, Price KP, Ellis J, Peijun S. 2003. Response of seasonal vegetation development to climatic variations in eastern central Asia. *Remote Sensing of Environment* **87**: 42–54. doi: 10.1016/s0034-4257(03)00144-5

Yu Y-S, Zou S, Whittemore D. 1993. Non-parametric trend analysis of water quality data of rivers in Kansas. *Journal of Hydrology* **150**: 61–80. doi: 10.1016/0022-1694(93)90156-4

Yue S, Wang CY. 2002. Applicability of prewhitening to eliminate the influence of serial correlation on the Mann–Kendall test. *Water Resources Research* **38**. doi: 106810.1029/2001wr000861

Zhang X, Ge Q, Zheng J. 2005. Impacts and lags of global warming on vegetation in Beijing for the last 50 years based on remotely sensed data and phonological information. *Shengtaixue Zazhi* **24**(2): 123–130.

Zhong L, Ma Y, Salama M, Su Z. 2010. Assessment of vegetation dynamics and their response to variations in precipitation and temperature in the Tibetan Plateau. *Climatic Change* **103**: 519–535. doi: 10.1007/s10584-009-9787-8

Zimmerman DW. 1986. Tests of significance of correlation coefficients in the absence of bivariate normal populations. *The Journal of Experimental Education* **54**: 223–227.

